Impurity behaviour in the ASDEX Upgrade divertor tokamak with large area tungsten walls

R. Neu, R. Dux, A. Geier, A. Kallenbach, R. Pugno, V. Rohde, D. Bolshukhin, J.C. Fuchs, O. Gehre, O. Gruber, J. Hobirk, M. Kaufmann, K. Krieger, M. Laux, C. Maggi, H. Murmann, J. Neuhauser, F. Ryter, A.C.C. Sips, A. Stäbler, J. Stober, W. Suttrop, H. Zohm and the ASDEX Upgrade Team

Max-Planck-Institut für Plasmaphysik, EURATOM Association, Boltzmannstr.2 D-85748 Garching , Germany

Abstract. At the central column of ASDEX Upgrade an area of 6.5 m^2 of graphite tiles was replaced tungsten coated tiles representing about two thirds of the total area of the central column. No negative influence on the plasma performance was found, except for ITB limiter discharges. The tungsten influx stayed below the detection limit except for direct plasma wall contact or a reduced clearance in divertor discharges. From these observations a penetration factor in the order of 1% and effective sputtering yields of about 10^{-3} could be derived, pointing to a strong contribution by light intrinsic impurities to the total W-sputtering. The tungsten concentrations ranged from below 10^{-6} up to a few times 10^{-5}. Generally, in discharges with increased density peaking, a tendency for increased tungsten concentrations or even accumulation was observed. Central heating (mostly) by ECRH led to a strong reduction of the central impurity content, accompanied by a very benign reduction of the energy confinement. The observations suggest that the W source strength plays only a inferior role for the central W content compared to the transport, since in the discharges with increased W-concentration neither an increase in the W influx nor a change in the edge parameters was observed. In contrast there is strong experimental evidence, that the central impurity concentration can be controlled externally by central heating.

PACS numbers: 52.25.Vy, 52.40.Hf, 52.55.Fa

1. Introduction

Although the plasma material interaction is strongly concentrated in the divertor region, it became rather evident in recent years, that in all divertor devices with large areas of carbon based wall components the carbon impurity household is strongly influenced by the main chamber carbon source. This was observed spectroscopically in ASDEX Upgrade [1, 2] as well as in JET [3] and also supported by erosion/deposition measurements in JET which were supplemented by model calculations [4]. Further confirmation for the important role of main chamber erosion follows from the JET Be-divertor experiment, where C still was the dominant impurity [3], as well as from the ASDEX Upgrade W divertor experiment [5], where no influence on the carbon concentration in the plasma bulk was observed and strong carbon deposits on the inner strike point modules were found after the campaign [6]. Taking these observations into account, the questions which arise when a metallic central column is used can be formulated as follows: How does the wall material itself influence plasma operation and performance and can the amount of migrating carbon be reduced by a significant factor? These questions are of essential importance for ITER, where Be is chosen as first wall material in the main chamber to avoid excessive codeposition of tritium with carbon [7]. In a later phase of ITER or in a DEMO reactor tungsten seems to be the only material at hand to stand the fluences with acceptable erosion [8]. Although W has large advantages over Be concerning thermo-mechanical properties, its use implies the risk of unduly high radiation losses in the central plasma. Except the high field tokamak Alcator C-Mod, where all plasma facing components (PFCs) consist of Mo (see for example [9] and references therein), there is no major fusion device using large areas covered by high-Z materials [10, 11].

In order to address the questions raised above, the central column of ASDEX Upgrade was covered with tungsten

coated graphite tiles in a step by step approach [12], based on the experience from the tungsten divertor experiment [5, 6]. During the experimental campaign 1999/2000 1.2 m^2 of the lower part of the central column were coated by tungsten. Regarding the erosion by CX particles, this region corresponds to the divertor baffles of ITER-FEAT, where the present design uses tungsten [8]. No negative influence on the plasma performance, even in high power H-modes or advanced discharge scenarios, was observed [13]. Mostly, it was not even possible to detect tungsten in the core plasma by spectroscopic methods, within a detection limit more than hundred times less than the maximum tolerable concentrations in ASDEX Upgrade. During the present campaign (April 2001 to July 2001) a total tungsten coverage of the central column was applied, except for regions, which may be hit directly by the shine through of the neutral beam injection (NBI) or which are used as a limiter. In Sec. 2 the setup of the W

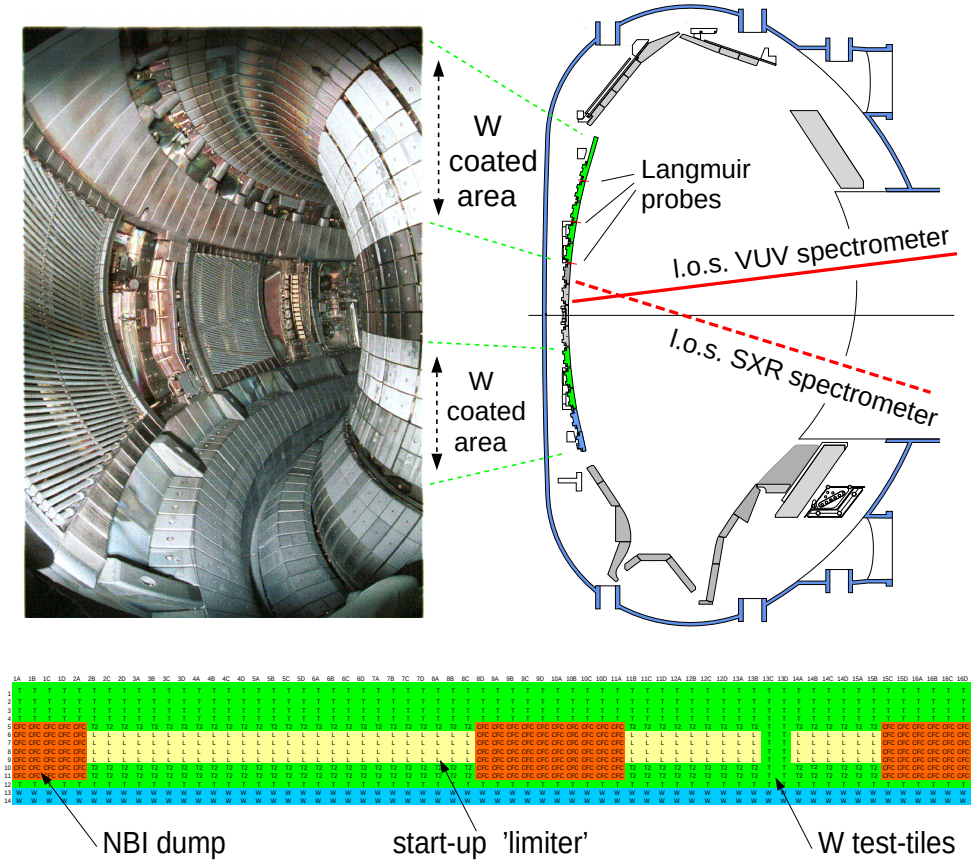

Figure 1. Left side: Tangential view of the central column of ASDEX Upgrade with the tungsten coated tiles. The four rows in the equatorial plane are made of graphite and CFC and are temporally used as limiter.
Right side: Poloidal cross section, showing the line of sights of the two main diagnostics for the central W radiation, as well as Langmuir probe tips installed at the central column.
Bottom: Schematic view of the unrolled central column: The light grey (green/blue) areas represent W coated tiles, the two lowest rows (blue) were already mounted in 1999. The dark grey (brown) tiles are manufactured from CFC because of potential shine through of the NBI. The white (yellow) tiles are ordinary graphite tiles. This central region of heat shield is used as limiter during the start-up phase of the discharge.

coverage and the experimental tools will be described, whereas the coating procedure and the detailed properties of the coating itself are presented elsewhere [14, 15]. The following section (Sec.3) deals with the behaviour of W in different discharge scenarios. The influence on the carbon content and the overall plasma performance is presented in Sec. 4 and finally, first conclusions are drawn in Sec. 5. The experimental campaign was finished as scheduled at the end of July 2001. Therefore, the detailed results of the post mortem studies of W-erosion and migration as well as on C deposition will be subject of a forthcoming paper [16].

2. Experimental setup

2.1. The tungsten coated central column

After the successful operation with two rows of W-coated tiles at the lower end of the heat shield (see Fig. 1, bottom) during the experimental campaign 1999/2000, it was decided to cover almost the full central column with tungsten [12]. At that time tests with direct plasma contact to tungsten could not be performed due to the low position of the W-tiles [13]. Therefore, the central region, which is used as limiter during plasma start-up and in L-mode internal transport barrier (ITB) discharges, was not coated with tungsten. The CFC tiles, used as dump for the shine-through of the NBI were also left out (see Fig. 1, bottom). Finally an area of 6.5 m^2 of coated tiles was installed (see Fig. 1). Additionally, two complete poloidal sets of W-coated tiles were mounted to analyze the tungsten erosion profile also at the limiter region. Before coating, the carbon tiles were shaped to reduce edge erosion. Unlike the tiles from 1999/2000, which were coated in-house by physical vapour deposition [14], the new tiles were coated commercially by plasma arc deposition to a thickness of 0.6-1.5 µm. They are characterized by a much brighter surface colour as the old ones at the bottom of the heat shield, which were kept from the the previous campaign (see Fig. 1, left side). Throughout the plasma operation of the campaign (4/2001 – 7/2001, ≈ 300 successful discharges) as well as in a first inspection during the scheduled vent, no failure of the coating was observed.

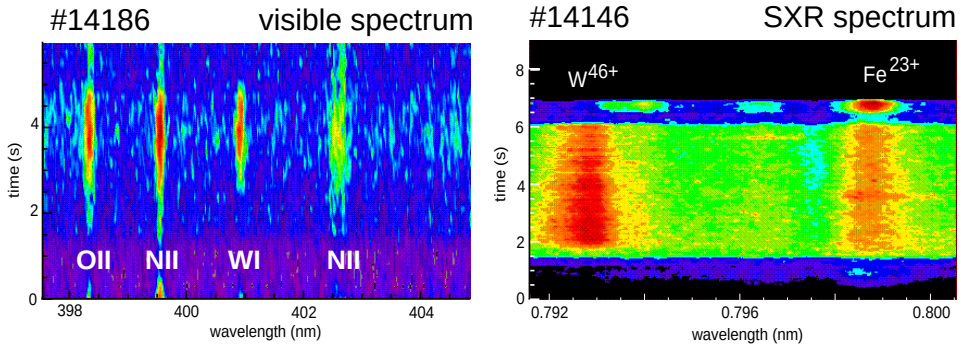

Figure 2. Temporal evolution of W spectra in the visible (left side, #14186) and in the soft X-ray spectral region (right side, #14146). The lowest intensity is marked in light grey (blue), whereas the highest one is plotted in dark grey (red).

2.2. Determination of the W-influxes and W-concentration

For the measurement of the W influx an array of 10 fiber guides is used, allowing the independent monitoring of every single row of W-tiles. The influx was determined from the brightness of the WI line at 400.8 nm using the inverse photon efficiency ($S/XB \approx 10$ at $T_e = 5$ eV) from [17]. The temporal evolution of the spectrum (#14186), measured during an R_{in} scan is shown on the left side of Fig.2. The tungsten concentration (c_W), which is relevant for the fusion performance, was determined using two different spectral signatures: The W-quasi-continuum, emitted from tungsten ions around W^{28+} in the vacuum ultra violet (VUV) at about 5 nm following the procedure described in [18], and a spectral line emitted from Ni-like tungsten (W^{46+}) in the soft X-ray spectral region (SXR) at 0.793 nm [19]. On the right side of Fig. 2 the temporal evolution of a high resolution spectrum measured with a Johann-spectrometer is shown for discharge #14146. Both diagnostics are cross calibrated using tungsten injections by laser blow off [13]. Using the spectra from ions with such different charge states guarantees a sensitive measurement of the central W-concentration for the usual range of central T_e in ASDEX Upgrade (1 - 5 keV). For $T_e > 2.5$ keV it even allows the extraction of some profile information of c_W.

3. Behaviour of tungsten in different discharge scenarios

The experimental campaign was started without additional wall conditioning by boronisation or siliconisation to run the plasma discharges with the pure tungsten surface. During this initial period the total radiation and the Z_{eff} were higher than for a good conditioned machine, but this was attributed to the high oxygen content (few percent). A dedicated program to investigate the performance of tungsten as plasma facing material was executed and all relevant scenarios were tested. After two weeks of operation, a boronisation was applied to reduce the oxygen content of the discharges.

3.1. Divertor discharges

3.1.1. Conventional H-Mode

The H-mode regime comprises by far the largest operational space in ASDEX Upgrade, since it is achieved at low densities ($\bar{n_e} \approx 4 \cdot 10^{19}$ m^{-3}) and intermediate toroidal fields $B_t \approx 2$ T for additional heating powers just above 1 MW [20, 21]. Therefore, most of the experimental data are gathered in the H-mode at low ($\delta \approx 0.15$) to intermediate ($\delta \leq 0.45$) triangularities. For low δ tungsten concentrations around 10^{-6} or below were observed. A typical example at intermediate density and heating power is shown in Fig. 3, performed still in the unboronised machine. The discharge shows very regular type I ELMs and sawteeth visible on T_{e0} and the soft X-ray brightness. All parameters, including c_W, quickly reach their flattop values and stay constant up to the pre-programmed discharge termination. The central tungsten concentration shows a strong correlation with the sawtooth activity and is always reduced by the sawtooth, very similar to the process described in detail in [22]. As can be judged from Fig. 2 on the right side, the spectroscopic signal for W is quite clear even though the low concentration of 10^{-6}, demonstrating the potential of the W detection in the soft X-ray spectral region. Although higher than with a boronised vessel – as mentioned above – the main chamber radiation is rather low (30%) and the confinement is good ($H_{ITER92Py} \approx 1$). Performing the same discharge at a higher density ($\bar{n_e} = 9 \cdot 10^{19}$ m^{-3}, $\bar{n_e}/n_{gw} = 0.75$) a fast decrease of c_W is observed during the density ramp until it falls below the detection limit [23].

In discharges with $\delta \approx 0.4$ the tungsten concentrations were higher by about a factor of five, reflecting the generally better particle confinement also seen for the natural density at a given current and heating power. Performing this kind of discharges with moderate constant gas-puffing at intermediate heating powers from NBI ($P_{NBI} \leq 7.5$ MW) yield a very high confinement at densities around or above the Greenwald limit. The reason for this seems to be a reduction of energy/particle transport in cases where the heating is applied further off axis as proposed by Stober et al. [24]. A further ingredient of these discharges is the slowly evolving density peaking of the background ions which could be explained by a very small inward velocity of the order of the neoclassical Ware-pinch [24]. Density peaking accompanied by weak temperature gradients are the natural prerequisites for neoclassical impurity accumulation, which amplifies the density peaking proportional to the charge of the impurities [25]. Therefore these discharges were prone to higher c_W reaching values above 10^{-5}, increasing during the whole discharge. To study this behaviour further, specially designed discharges were performed. From the tungsten divertor experiment the tendency of tungsten accumulation for low voltage NBI, i.e. off axis heated discharges is known [5]. Therefore the NBI energy was reduced from 60 keV to $35-40$ keV, to shift the heating profile further off-axis. In these discharges the tungsten concentration rises after switching on the beams, until the sawteeth were lost and extremely peaked electron profiles were observed, finally leading to central tungsten concentrations of up to $4 \cdot 10^{-5}$ [23]. Performing the same discharge with full beam voltage, i.e. more central heating, c_W stays around 10^{-6}. An even clearer experimental proof is provided using central ECRH: switching on the ECRH during the evolving accumulation, a fast suppression is found [23]. The effect is even clarified after switching off the ECRH heating, when the tungsten concentration rises again. The experiment was also performed by an exact replacement of beam power against ECRH power, to exclude the confinement degradation by additional heating power. This discharge showed the same beneficial behaviour. The mechanism appears to be a complex interplay of the anomalous transport of the background ions and the anomalous and neoclassical transport of tungsten. However, experimentally it could

clearly be shown, that the central tungsten concentration can be controlled externally by central heating.

A significant amount of tungsten influx was only measured during plasma start-up and in special designed

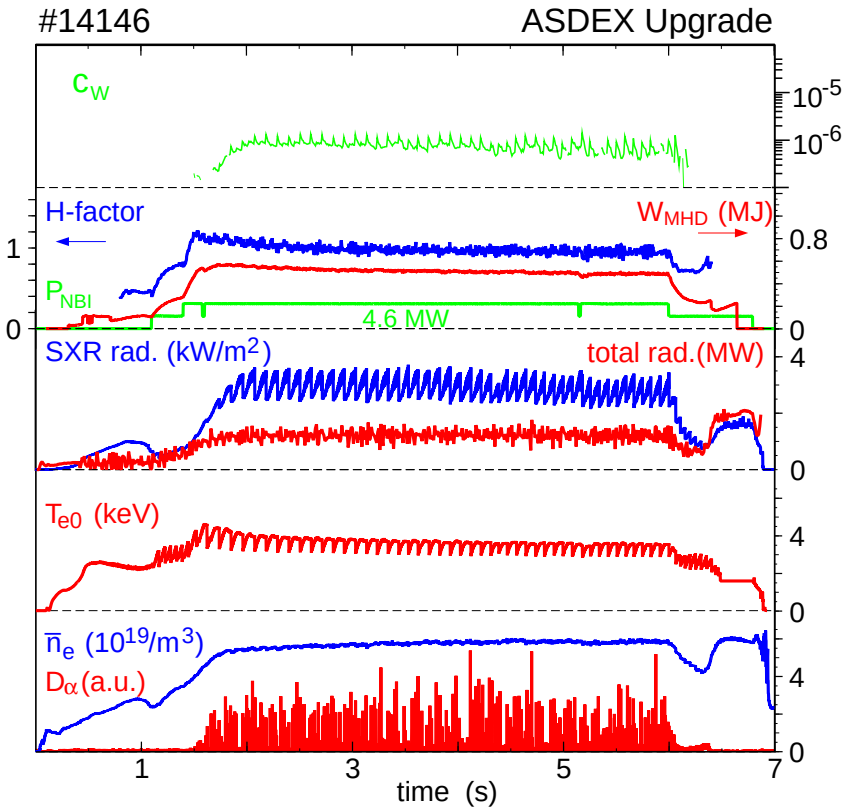

Figure 3. Typical H-mode discharge at 1 MA and intermediate density and heating power, performed before boronisation. The H-factor is calculated according to the ITER92P ELMy H-mode scaling and the tungsten concentration (c_W) is extracted from the central line emission of W^{46+}.

discharges, which had low clearance with respect to the tungsten tiles (or when using the tungsten tiles as limiter, see Sec. 3.2). Fig. 4 shows the behaviour of the W-influx (Γ_W) and the W-concentration (c_W) during a radial shift of the plasma towards the central column in discharge #14186 ($I_p = 1$ MA, $B_t = -2.3$ T, $P_{NBI} = 5$ MW, $\delta = 0.15$). As can be judged from the top traces on the left ($\bar{n}_e$, T_{e0}), the main plasma parameters remain constant during the shift. At the nominal clearing of 12 cm to the inner wall, no influx above the detection limit is evident. During the shift the influx rises to a maximum value of $3 \cdot 10^{18} \mathrm{m}^{-2} s^{-1}$ for the lowest clearance of 4 cm. The increase of the W I brightness is only seen on the W-coated tile which is nearest to the equatorial plane, in line with the equilibrium reconstruction. Therefore one can assume that only a ring with approximately the height of one tile ($\pm 50\%$) contributes significantly to the influx. Taking into account that only about the half of the circumference is erosion dominated [26], this results in an area of 0.33 m^2 where W is eroded and consequently a total W-influx of $\approx 10^{18}$ s^{-1} from this row. This has to be taken as a lower boundary, since it is to be expected that the W-influx from the other rows with W-tiles is also increased, although below the detection limit. However looking at the clear signal for W I for this discharge in Fig.2, it is evident that the remaining increase of the W-flux would at maximum of the same size as the measured one. The detectable increase of the influx points clearly to the fact that the plasma in the far scrape-off layer is hot enough to lead to W-erosion (see [27]). When calculating the D-flux to the wall by using the brightness of the simultaneously measured D_δ and $S/XB = 6000$ one can even derive an effective sputtering yield $Y_W^{eff} \approx 10^{-3}$. Obviously this can not be due to pure D sputtering since this would result in ion temperatures in the range of 100 eV. But taking into account sputtering by a few percent of light impurity ions (O, C), temperatures in the range of 10 eV would be sufficient [6, 11] to yield a consistent result.

In parallel to the increased influx, an increase of the W-concentration is observed. Assuming spatially constant c_W one gets for the increase from $1 \cdot 10^{-6}$ to $2 \cdot 10^{-6}$van additional inventory of $\Delta N_W = N_e \cdot \Delta c_W \approx 8 \cdot 10^{14}$ W-ions. Since the W concentration during the phase with standard clearance, was $\approx 1 \cdot 10^{-6}$ one can derive there an W-influx of the same absolute size as from the single row during the shift, however the flux density must be lower by the ratio of active surfaces, namely by about a factor of 20, consistent with the detection limit of the diagnostic. The ratio $\Delta N_W / \Delta \Gamma_W$ gives the particle confinement time $\tau_p = 8 \cdot 10^{14} / 10^{18} = 0.8$ ms. To compare this number to earlier results [13] and investigations in other machines one can separate τ_p in a penetration probability f (sometimes also called screening), that means the probability to reach the confined plasma, and the transport time τ_t within the confined plasma. Taking $\tau_t = \tau_E \approx 100$ ms one gets $f = 0.8\%$ as an upper estimate, since usually τ_t is somewhat larger than τ_E and $\Delta \Gamma_W$ was the lower boundary. This value is lower than $f = 3\%$ from [13] where it was deduced from laser blow-off experiments, which may lead to the injection of clusters penetrating more easily. The value is also almost a factor of 10 lower than the results from screening experiments with methane measured for top fueling of methane in JET [28, 29] but similar to nitrogen puffing experiments at the central column in Alcator C-Mod [30].

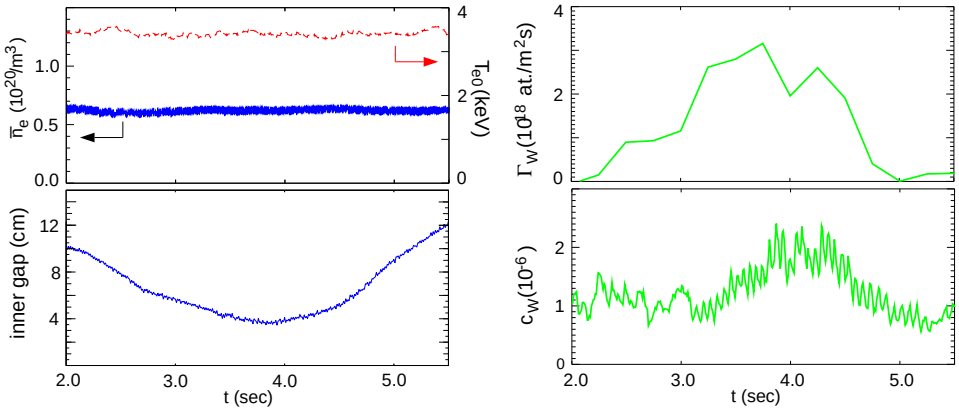

Figure 4. Behaviour of the W-influx (Γ_W) and the W-concentration (c_W) during the radial shift of the plasma towards the central column in discharge #14186 ($I_p = 1$ MA, $B_t = -2.3$ T, $P_{NBI} = 5$ MW, $\delta = 0.15$). On the top $\bar{n}_e$ and T_{e0} are shown, to demonstrate that the main plasma parameters remain constant during the shift.

*3.1.2. Improved H-Modes, ITB- and high-*β *discharges*

Advanced scenarios are the second important experimental topic at ASDEX Upgrade. Especially improved H-modes, which are characterized by fishbone instead of sawtooth activity, no central barrier but generally improved confinement over ordinary H-modes are given some emphasis since they can be performed in quasi steady-state [31]. This kind of discharges were already tested with an unboronised vessel at the beginning of the campaign. Since the overall conditioning of the machine was not sufficient, the plasma density was slightly too high and the best performance values of [31] were not reached. The tungsten concentrations extracted in these discharges, show similar values and characteristics as ordinary low density H-modes.

An enlargement of the operational space for the improved H-mode towards higher densities was gained by running the discharges at $\delta \approx 0.4$ [32]. As in ordinary H-modes at medium to high triangularity discharges, the tungsten concentration showed the tendency to increase slowly throughout the whole duration of the discharge to values of about $c_W \approx 10^{-5}$. This evolution was accompanied by an increasing density peaking as already described in Sec. 3.1.1. To test the applicability of the method of central heating for the reduction of the central impurity confinement, central ECRH was applied during the flattop phase of a discharge as shown in Fig. 5. The initial very good confinement was not sustained, nevertheless the H-factor stayed above 1.1. From $t \approx 1.8$ s the W-concentration rises continuously and shortly after $t \approx 2.2$ s the soft-X ray measurement saturates. It has to be pointed out that this increase in the SXR brightness is not exclusively due to the increase of the W density, since also the brightness of other impurity radiation (for example Fe) is also found to rise. From $t = 3.0$ s on central ECRH is

added (first 1.4 MW, after about 200 ms 0.8 MW; note the power is in the same scale as the NBI power). During the ECRH phase, T_{e0} is increased but no (or very minor) sawteeth appear and $\bar{n}_e$ is slightly decreased similar to the so-called density pump out effect described in [33]. The stored energy stayed almost constant leading to a slight reduction of the H factor from 1.14 to 1.06. However, the by far strongest effect is found on the SXR brightness and the tungsten concentration. Both drop on the timescale of the energy confinement time, leading to c_W below 10^{-6}. In Fig. 6 (left side), the radial extension of the fractional abundance of W^{46+} is shown, demonstrating that in both phases of the discharge the spectroscopic measurement is sensitive to the central W-content. After the heating phase again a rapid increase of the SXR brightness and c_W is observed.

Since the edge parameters are unchanged throughout the discharge, large variation of the W-source are very unlikely (in fact the are below the detection limit). Therefore, the behaviour may be explained within the framework of the picture, already discussed in Sec. 3.1.1. Coupled to the low energy transport in these discharges the anomalous particle transport is also decreased, allowing that even a very small drift velocity leads to a density peaking as shown in Fig. 6, right side. This density peaking together with low anomalous transport and a moderate peaking of the temperature profiles provokes the neoclassical impurity accumulation. The central wave heating obviously counteracts this in several ways. The anomalous particle transport is increased, leading to flatter density profiles of the background ions (the hollow density profile measured by Thomson scattering during the ECRH has still to be validated by other measurements). At the same time T_{e0} and therefore also the gradient is increased. Assuming a fast equilibration of T_e and T_i, this then leads to a strong reduction of the neoclassical inward drifts. Together with the increased anomalous transport this results in a strong reduction of the central impurity content. Clearly, these model assumptions have still to be verified by detailed calculations, which are under way.

In parallel to the improved H-Mode discharges, other routes to advanced tokamak observation were pursued,

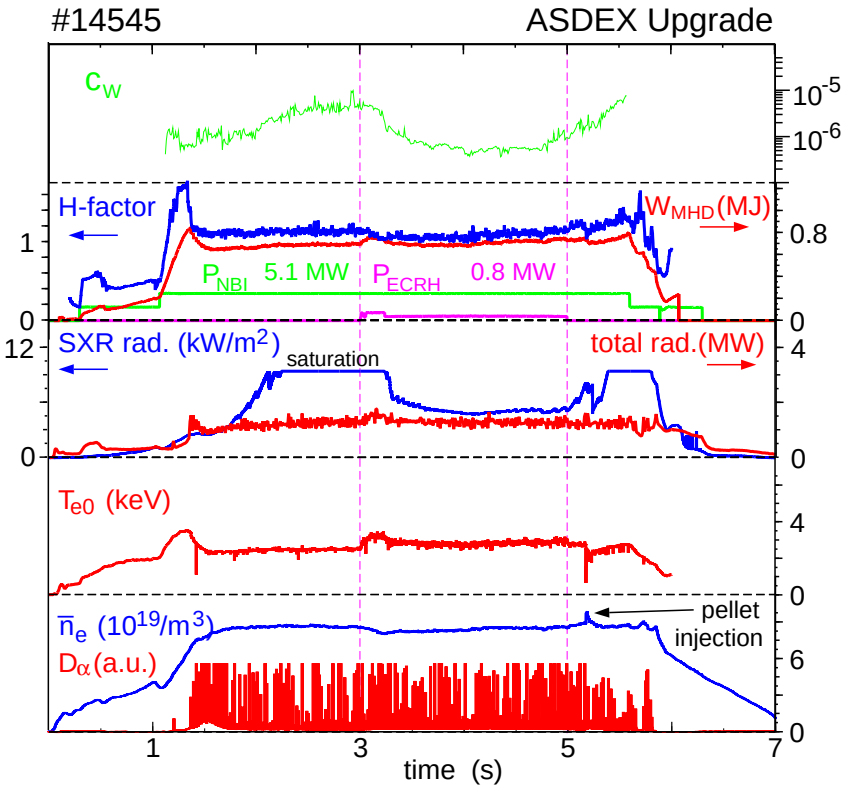

Figure 5. Moderately improved H-mode discharge at $I_p = 1$ MA, $B_t = -2.5$ T, $\delta = 0.4$, showing enhanced c_W with NBI only, but a strong reduction of c_W during central ECRH. Note the scales are the same as in Fig.3 except for the density and SXR brightness.

namely high-β discharges as well as discharges with electron ITBs. In both cases the highest performances were

obtained during this campaign and the detailed results will be presented elsewhere [34, 35]. From the viewpoint of the tungsten contamination, they were completely unaffected and c_W stayed mostly below the detection limit of the VUV as well as the SXR diagnostics.

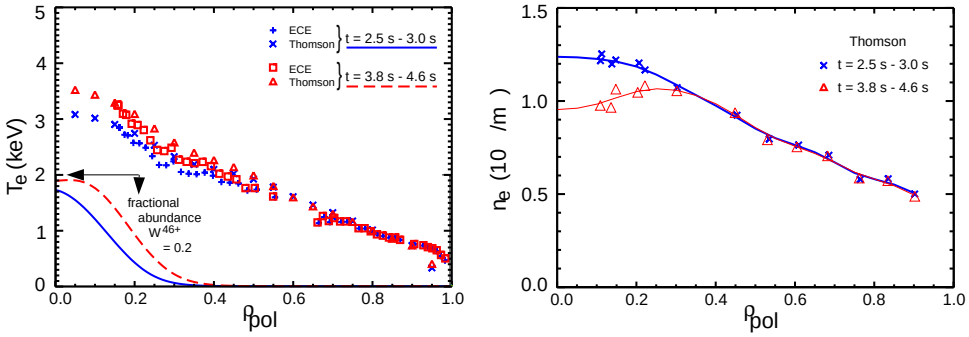

Figure 6. Electron temperature and density profiles of discharge #14545 before and during central ECRH (The solid lines represent a fit through the experimental density data). The fractional abundance for W^{46+}, which is used to calculate the W concentration, is also shown in the left part.

3.2. Limiter discharges

There are several examples for the use of tungsten as limiter available in literature (see [36, 10] and references therein) and the early results from PLT [37] showing strong central impurity accumulation for certain circumstances had a strong negative impact on the further use of tungsten in fusion devices.
Limiter discharges play a very minor role in the experimental program of ASDEX Upgrade. Conventional L-modes were only of operational interest, in order to explore their behaviour in regard to a future plasma start-up at a fully tungsten covered central heat shield. The other range of use is to force discharges to an L-mode edge even at heating powers which lie considerably above the L-H transition threshold in order to explore ITB discharges with L-mode edge. Common to these discharges is the impact of high energy ions to the tungsten surfaces, which results in increased W-erosion and W-influx. Due to direct contact of W-flux to the last closed flux surface (LCFS) its penetration to the confined region is also more likely.

3.2.1. Conventional L-mode

To explore the influence of the plasma wall interaction with tungsten surfaces in limiter configurations, several discharges at intermediate densities, ohmic as well as with additional heating powers up to 5 MW were performed. During these discharges the plasma was shifted vertically towards the tungsten tiles. As expected, the W-concentration increased during the plasma contact with W surfaces to values around 10^{-5}. However no serious accumulation was observed for the discharge parameters considered.

3.2.2. ITB discharges with L-mode edge

A common scenario with an internal transport barrier on ASDEX Upgrade uses the heat shield as limiter in order to maintain L-mode edge. In discharge #14274, which was performed already after the first boronisation, the central tungsten concentration rises as soon as the LCFS is in contact with the tungsten heat shield (0.7 s), as indicated in Fig. 7. It exhibits a short weak transport barrier (0.8 - 0.9 s), which results in tungsten accumulation to values above the saturation level of the detector. Due to the finite transport time the highest c_W-values were reached shortly after. After the decay of the ITB the central tungsten concentration drops again and the onset of sawteeth results in a further reduction. Although being a limiter discharge further on the plasma completely recovers from

the former high tungsten concentrations and reaches tolerable tungsten concentrations. After switching off one of the beams, the core temperature dropped below 2 keV and was too low to extract c_W from the SXR radiation.
In general, the limiter ITB scenario resulted in the highest tungsten concentrations measured during the campaign. For discharges with stronger transport barriers even concentrations above $3 \cdot 10^{-4}$ were measured. Since all of the these discharges were performed at the same density with an L-mode edge it is reasonable to assume that the edge plasma and therefore the tungsten source did not change throughout the discharge. This leads again to the conclusion that the strong variation of the central tungsten concentration can only be explained by the strong variation of the transport of the background ions and the impurity ions in the core plasma. This kind of discharge is only seen as an interim solution for better suited divertor discharges. Consequently, no efforts were undertaken to optimize the impurity behaviour using central wave heating.

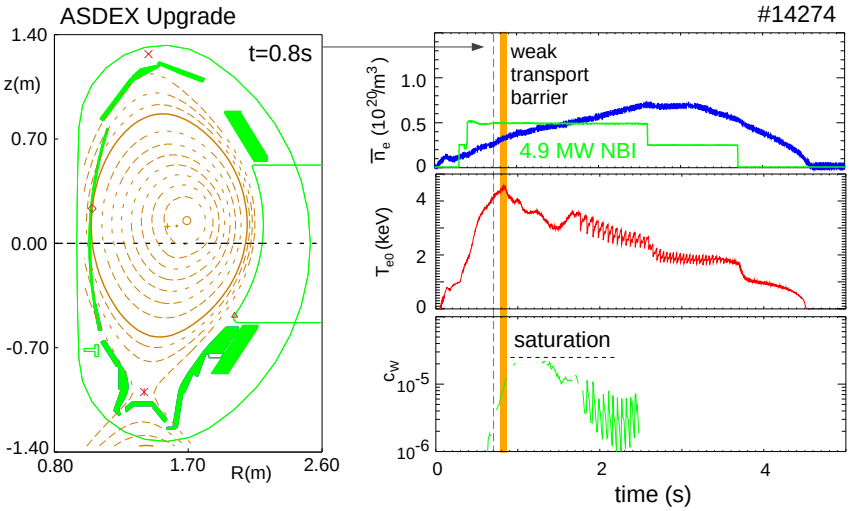

Figure 7. Limiter discharge with weak internal transport barrier showing tungsten accumulation. After the collapse of the barrier the central tungsten concentration drops.

4. Carbon content and plasma performance

One of the primary questions was, whether the carbon content and the resulting carbon deposits can be reduced by using a large area metal wall. Although two thirds of the central column, which is assumed to be one of the strongest carbon sources, are covered with tungsten, it has to be kept in mind that other surfaces (divertor, passive stabilizer loops) still represent a much larger area with carbon based PFCs, as can be judged from Fig. 1. Therefore only small changes in the central carbon content are to be expected. Fig. 8 shows the long term behaviour of the C VI Lyman-α brightness $I_{C\,VI}$ in 'standard' H-mode discharges. The campaign 2001 comprises the discharges from $\approx 14100 - 14600$. A long term decrease seems to be visible especially since the regular application of the siliconisation. Although no siliconisation was applied during the campaign 2001 and large areas of new graphite surfaces were introduced during the preceding vent (installation of the new divertor IIb, see [20]) $I_{C\,VI}$ is at the lower end of the observed range right after the first boronisation, pointing to some carbon reduction due to the W-coatings. This interpretation is supported by the temporal behaviour, showing the lowest brightnesses right after the start of the campaign and an increase throughout, which might be explained by migrating carbon. Additionally the reduction of $I_{C\,VI}$ is more obvious for the high density phase of discharges ($\bar{n}_e \approx 10^{20}$ m^3, diamonds) in agreement with the interpretation that under such discharge conditions chemical erosion from a graphite heat shield should be maximal, in contrast to the low density phase ($\bar{n}_e \approx 4 - 5 \cdot 10^{19}$ m^3, crosses) where physical sputtering in the divertor may be dominant. Further information on the behaviour of carbon will be gained from charge exchange

recombination spectroscopy, where the absolute calibration is in progress. The post mortem analyses of the erosion of W and the deposition of migrated C [16] will help to check the consistency of the picture.

There was no strong impact of the tungsten coated wall on the general plasma behaviour as already indicated in

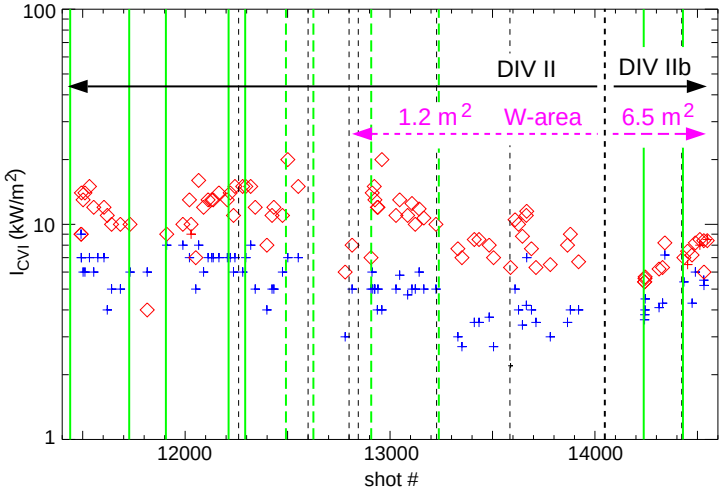

Figure 8. Long term behaviour of the C VI Lyman-α brightness in 'standard' H-mode discharges ($I_p = 1$ MA, $B_t = -2.0$ T, $P_{NBI} = 5$ MW, $\delta = 0.15$) at low (crosses) and high (diamonds) densities. The vertical lines represent vents (short dashed) boronisation (solid) and siliconisation (long dashed).

Sec. 3, except for the ITB discharges with L-Mode edge. The only obvious difference to previous campaigns was the significant reduction of the H-mode threshold by 20% measured also in the 'standard' H-mode discharge [21, 20]. However whether this reduction is related to the tungsten coated heat shield or, what seems more likely, to changes in the edge plasma due to the modified divertor, is not clarified yet.

5. Conclusions and Outlook

Two thirds of the area of the central column of ASDEX Upgrade were covered with tungsten coated tiles. Due to the large surface, a sensitive check of the influence of tungsten as a plasma facing material in the main chamber on the plasma performance under fusion reactor relevant conditions could be performed. No negative influence on the plasma performance was found, except for ITB limiter discharges. The experimental indication for the reduction of the the carbon content in the plasma has still to be validated by other measurements.

The tungsten influx stayed below the detection limit except for direct plasma wall contact or a reduced clearance in divertor discharges. From these observations a penetration factor in the order of 1% and effective sputtering yields of about 10^{-3} could be derived, pointing to a strong contribution by light intrinsic impurities. The tungsten concentrations ranged from below 10^{-6} up to a few times 10^{-5}. Generally, in discharges with increased or/and evolving density peaking, a tendency for increased tungsten concentrations or even accumulation was observed. Central heating (mostly) by ECRH led to a strong reduction of the central impurity content, accompanied by a very modest reduction of the energy confinement. The observations suggest that the W source strength plays only a inferior role for the central W content compared to the transport, since in the discharges with increased W-concentration neither an increase in the W influx (always below detection limit) nor a change in the edge parameters were observed. These findings are also in line with the results from the W divertor experiment [38, 39]. The mechanism behind seems to be a complex interplay of anomalous transport of the background ions and the anomalous and neoclassical transport of tungsten. Coupled transport analyses for background ions as well as for the impurities are under way but since they need a very sophisticated data evaluation and validation, they are not completed yet and have to presented in a forthcoming paper. However, experimentally it could clearly be shown, that the central tungsten concentration can be controlled externally by central heating.

The experiences made during the campaign 2001 showed, that the operational space is somewhat more restricted than for a device having only low-Z PFCs. However, W could also be thought as a sensitive marker for discharge scenarios which are intrinsically prone to impurity accumulation and consequently will be only of very restricted ITER relevance. Therefore the conclusion was drawn that further parts of the heat shield will be coated during the vent of autumn 2001 leaving only a smaller number CFC tiles uncoated. This will lead to a sensitive check to which degree the breakdown is modified moving from a low Z start-up limiter to a high-Z PFC. Moreover it is foreseen to coat other large areas with graphite tiles (such as the PSL with another 10 m^2) on the way to a fully tungsten coated fusion device.

References

[1] A. Kallenbach, R. Neu, W. Poschenrieder, and ASDEX Upgrade Team, *Nucl. Fusion* 34, 1557 (1994).

[2] R. Pugno, A. Kallenbach, D. Bolshukhin, R. Dux, J. Gafert, R. Neu, V. Rohde, K. Schmidtmann, W. Ullrich, U. Wenzel, and ASDEX Upgrade Team, *J. Nucl. Mater.* 290–293, 308 (2001).

[3] G. McCracken et al., *Nucl. Fusion* 39, 41 (1999).

[4] J. Coad, N. Bekris, J. Elder, S. Erents, D. Hole, K. Lawson, G. Matthews, R.-D. Penzhorn, and P. Stangeby, *J. Nucl. Mater.* 290 – 293, 224 (2001).

[5] R. Neu, K. Asmussen, K. Krieger, A. Thoma, H.-S. Bosch, S. Deschka, R. Dux, W. Engelhardt, C. García-Rosales, O. Gruber, A. Herrmann, A. Kallenbach, M. Kaufmann, V. Mertens, F. Ryter, V. Rohde, J. Roth, M. Sokoll, A. Stäbler, W. Suttrop, M. Weinlich, H. Zohm, M. Alexander, G. Becker, K. Behler, K. Behringer, R. Behrisch, A. Bergmann, M. Bessenrodt-Weberpals, M. Brambilla, H. Brinkschulte, K. Büchl, A. Carlson, R. Chodura, D. Coster, L. Cupido, H. J. de Blank, S. De Peña Hempel, R. Drube, H.-U. Fahrbach, J.-H. Feist, W. Feneberg, S. Fiedler, P. Franzen, J. C. Fuchs, G. Fußmann, J. Gafert, O. Gehre, J. Gernhardt, G. Haas, G. Herppich, W. Herrmann, S. Hirsch, M. Hoek, F. Hoenen, F. Hofmeister, H. Hohenöcker, D. Jacobi, W. Junker, O. Kardaun, T. Kass, H. Kollotzek, W. Köppendörfer, B. Kurzan, K. Lackner, P. T. Lang, R. S. Lang, M. Laux, L. L. Lengyel, F. Leuterer, M. E. Manso, M. Maraschek, K.-F. Mast, P. McCarthy, D. Meisel, R. Merkel, H. W. Müller, M. Münich, H. Murmann, B. Napiontek, G. Neu, J. Neuhauser, M. Niethammer, J.-M. Noterdaeme, E. Pasch, G. Pautasso, A. G. Peeters, G. Pereverzev, C. S. Pitcher, W. Poschenrieder, G. Raupp, K. Reinmüller, R. Riedl, H. Röhr, H. Salzmann, W. Sandmann, H.-B. Schilling, D. Schlögl, H. Schneider, R. Schneider, W. Schneider, G. Schramm, J. Schweinzer, B. D. Scott, U. Seidel, F. Serra, E. Speth, A. Silva, K.-H. Steuer, J. Stober, B. Streibl, W. Treutterer, M. Troppmann, N. Tsois, M. Ulrich, P. Varela, H. Verbeek, P. Verplancke, O. Vollmer, H. Wedler, U. Wenzel, F. Wesner, R. Wolf, R. Wunderlich, D. Zasche, T. Zehetbauer, and H.-P. Zehrfeld, *Plasma Phys. Controlled Fusion* 38, A165 (1996).

[6] K. Krieger, H. Maier, R. Neu, and ASDEX Upgrade Team, *J. Nucl. Mater.* 266–269, 207 (1999).

[7] G. Federici, J. Brooks, D. Coster, G. Janeschitz, A. Kukuskhin, A. Loarte, H. Pacher, J. Stober, and C. Wu, *J. Nucl. Mater.* 266-269, 260 (2001).

[8] G. Janeschitz, ITER JCT, and ITER HTs, *J. Nucl. Mater.* 290 – 293, 1 (2001).

[9] B. Lipschultz, D. Pappas, B. LaBombard, J. Rice, D. Smith, and S. Wukitch, *Nucl. Fusion* 41, 585 (2001).

[10] N. Noda, V. Philipps, and R. Neu, *J. Nucl. Mater.* 241 – 243, 227 (1997).

[11] V. Philipps, R. Neu, J. Rapp, U. Samm, M. Tokar, T. Tanabe, and M. Rubel, *Plasma Phys. Controlled Fusion* 42, B293 (2000).

[12] V. Rohde, R. Neu, K. Krieger, H. Maier, A. Geier, A. Tabasso, A. Kallenbach, R. Pugno, D. Bolshukhin, M. Zarrabian, and ASDEX Upgrade Team, Operation of ASDEX Upgrade with High-Z Wall Coatings, in *Plasma Physics and Controlled Nuclear Fusion Research ...*, volume 0, pp. –, Vienna, 2000, IAEA.

[13] R. Neu, V. Rohde, A. Geier, K. Krieger, H. Maier, D. Bolshukin, A. Kallenbach, R. Pugno, K. Schmidtmann, M. Zarrabian, and ASDEX Upgrade Team, *J. Nucl. Mater.* 290–293, 206 (2001).

[14] H. Maier, J. Luthin, M. Balden, M. Rehm, F. Koch, and H. Bolt, *J. Nucl. Mater.* 142-144, 733 (2001).

[15] H. Maier, J. Luthin, M. Balden, J. Linke, V. Rohde, and H. Bolt, Development of tungsten coatings for plasma-facing components and their application in ASDEX Upgrade, in *Proc. of the 10th Int. Conference on Fusion Reactor Materials, Baden-Baden, Germany*, 2001.

[16] K. Krieger, V. Rohde, J. Roth, W. Schneider, and ASDEX Upgrade team, Erosion and migration of tungsten employed at the central column heat shield of ASDEX Upgrade, in *Proc. of the 10th Int. Conference on Fusion Reactor Materials, Baden-Baden, Germany*, 2001.

[17] J. Steinbrink, U. Wenzel, W. Bohmeyer, G. Fußmann, and PSI Team, Sputtered Tungsten Atoms Investigated in a Linear Plasma Generator, in *Europhysics Conference Abstracts (Proc. of the 24th EPS Conference on Controlled Fusion and Plasma Physics, Berchtesgaden, 1997)*, 1997.

[18] K. Asmussen, K. B. Fournier, J. M. Laming, R. Neu, J. F. Seely, R. Dux, W. Engelhardt, J. C. Fuchs, and ASDEX Upgrade Team, *Nucl. Fusion* 38, 967 (1998).

[19] R. Neu, K. Fournier, D. Bolshukhin, and R. Dux, *Physica Scripta* T92, 307 (2001).

[20] R. Neu et al., Properties of the new Divertor IIb in ASDEX Upgrade, in *Proc. IAEA TCM on Divertor Concepts, Aix en Provence, France, 2001*, Vienna, 2001, IAEA.

[21] F. Ryter et al., Survey of H-Mode L-H Transition and Confinement from ASDEX Upgrade H-Mode Standard Shot, in *Proc. IAEA TCM*

on H-Mode Physics and Transport Barriers, Toki, Japan, 2001, Vienna, 2001, IAEA.

[22] R. Dux, A. G. Peeters, A. Gude, A. Kallenbach, R. Neu, and ASDEX Upgrade Team, *Nucl. Fusion* 39, 1509 (1999).

[23] V. Rohde et al., Tungsten as first wall material in the main chamber of ASDEX Upgrade, in *Europhysics Conference Abstracts (CD-ROM), Proc. of the 28th EPS Conference on Controlled Fusion and Plasma Physics, Funchal, 2001*, Geneva, 2001, EPS.

[24] J. Stober et al., *to be published in Plasma Phys. Control. Fusion* (2001).

[25] G. Fussmann, A. Field, A. Kallenbach, K. Krieger, K. Steuer, and ASDEX-TEAM, *Plasma Phys. Controlled Fusion* 33, 1677 (1991).

[26] W. Schneider et al., Tungsten Migration between Main Chamber and Divertor of ASDEX Upgrade, in *Europhysics Conference Abstracts (Proc. of the 28th EPS Conference on Controlled Fusion and Plasma Physics, Funchal, 2001)*, 2001.

[27] J. Neuhauser et al., Transport into and across the scrape-off layer in the ASDEX Upgrade divertor tokamak, in *Proc. IAEA TCM on Divertor Concepts, Aix en Provence, France, 2001*, Vienna, 2001, IAEA.

[28] J. Strachan, W. Fundamenski, M. Charlet, K. Erents, J. Gafert, C. Giroud, M. von Hellermann, G. Matthews, et al., Screening of Hydrocarbon Sources in JET, in *Europhysics Conference Abstracts (Proc. of the 28th EPS Conference on Controlled Fusion and Plasma Physics, Funchal, 2001)*, 2001.

[29] A. Stamp, D. Elder, H. Guo, M. von Hellermann, L. Horton, R. König, J. Lingertat, G. McCracken, A. Meigs, P. Stangeby, and A. Tabasso, *J. Nucl. Mater.* 266-269, 685 (1999).

[30] G. McCracken, R. Granetz, B. Lipschultz, B. LaBombard, F. Bombarda, J. Goetz, S. Lisgo, D. Jablonski, H. Ohkawa, J. Rice, P. Stangeby, J. Terry, and Y. Wang, *J. Nucl. Mater.* 241 – 243, 777 (1997).

[31] O. Gruber, R. C. Wolf, R. Dux, C. Fuchs, S. Günter, A. Kallenbach, K. Lackner, M. Maraschek, P. J. McCarthy, H. Meister, G. Pereverzev, F. Ryter, J. Schweinzer, U. Seidel, S. Sesnic, A. Stäbler, J. Stober, and ASDEX Upgrade Team, *Phys. Rev. Lett.* 83, 1787 (1999).

[32] A. Sips et al., in *Proc. IAEA TCM on H-Mode Physics and Transport Barriers, Toki, Japan, 2001*, Vienna, 2001, IAEA.

[33] F. Ryter, J. Stober, A. Stäbler, G. Tardini, H.-U. Fahrbach, O. Gruber, A. Herrmann, A. Kallenbach, M. Kaufmann, B. Kurzan, F. Leuterer, M. Maraschek, H. Meister, A. G. Peeters, G. Pereverzev, A. C. C. Sips, W. Suttrop, W. Treutterer, H. Zohm, and ASDEX Upgrade Team, *Nucl. Fusion* 41, 537 (2001).

[34] A. Sips et al., in *Proc. IAEA TCM on H-Mode Physics and Transport Barriers, Toki, Japan, 2001*, Vienna, 2001, IAEA.

[35] R. Wolf et al., in *Proc. IAEA TCM on H-Mode Physics and Transport Barriers, Toki, Japan, 2001*, Vienna, 2001, IAEA.

[36] A. Pospieszczyk, T. Tanabe, V. Philipps, G. Sergienko, T. Ohgo, K. Kondo, M. Wada, M. Rubel, W. Biel, A. Huber, A. Kirschner, J. Rapp, and N. Noda, *J. Nucl. Mater.* 290–293, 947 (2001).

[37] V. Arunasalam, C. Barnes, K. Bol, K. Brau, N. Bretz, M. Brusati, S. Cohen, S. Davis, D. Dimock, F. Dylla, D. Eames, P. Efthimion, H. Eubank, H. Furth, R. Goldston, R. Hawryluk, K. Hill, E. Hinnov, R. Horton, J. Hosea, H. Hsuan, D. Ignat, F. Jobes, D. Johnson, M. Mattioli, E. Mazzucato, E. Meservey, P. Moriette, N. Sauthoff, J. Schivell, G. Schmidt, R. Smith, F. Stauffer, W. Stodiek, J. Strachan, S. Suckewer, and S. von Goeler, Recent Results from the PLT tokamak, in *Proc. 8th Conf. EPS, Prague 1977*, volume 2, pp. 17–28, Geneva, 1978, EPS.

[38] K. Asmussen, R. Neu, R. Dux, W. Engelhardt, K. Fournier, J. C. Fuchs, K. Krieger, J. Rice, V. Rohde, D. Schlögl, M. Sokoll, A. Thoma, and ASDEX Upgrade Team, Investigations of Tungsten in the Central Plasma of ASDEX Upgrade, in *Europhysics Conference Abstracts (Proc. of the 24th EPS Conference on Controlled Fusion and Plasma Physics, Berchtesgaden, 1997)*, edited by M. Schittenhelm, R. Bartiromo, and F. Wagner, volume 21A, part IV, pp. 1393–1396, Petit-Lancy, 1997, EPS.

[39] A. Geier, Aspekte des Verhaltens von Wolfram im Fusionsexperiment ASDEX Upgrade, Technical Report 10/19, IPP, Garching, Germany, 2001.